Modeling and Design of a Soft Reconfigurable Microrobot

E.W. van den Brink* and Islam S. M. Khalil

University of Twente, Faculty of Engineering Technology
Drienerlolaan 5, 7522 NB, Enschede, The Netherlands
**e.w.vandenbrink@student.utwente.nl*

ABSTRACT: In this paper, a reconfigurable microrobot, which is referred to as MagTwist, is modeled and designed. MagTwist consists of a flat sheet with magnetic moment at its proximal and distal ends, with opposite polarities. This tetherless device has the capability to swim in a controllable manner. Therefore, it has the potential to access small spaces in a versatile and noninvasive manner and mitigates the negative side-effects associated with conventional medical procedures. When a magnetic field is applied, magnetic torques are exerted on its opposite dipole moments and the soft body undergoes elastic deformation about its long axis. When rotating the shape produces a propulsion force. A numerical model is derived and used to predict the velocity of the microrobot at low Reynolds numbers when the magnetic field rotates. It is based on the regularized stokeslets (RST). The achieved maximum velocity is 17.7 mm/s. This RST-Based model predicts the ideal twist angle and geometry. To ensure the optimal angle of twist of 180° at 20 mT is achieved, the length should be approximately 3 mm and the thickness 0.1 mm. To maximize velocity, a width of 1.2 mm is found. A high cut-off frequency is achieved by using a fluid with a viscosity of 0.001 Pas. The RST model is compared to a model based on the resistive-force theory (RFT) and both models correspond.

Key words: microrobot, magnetic, reconfigurable, regularized stokeslets, resistive-force theory, soft, tetherless

1 INTRODUCTION

In minimally invasive surgery, various procedures require medical tools to be inserted in the body of the patient. However, this method comes with various implications and difficulties, such as the inability to reach certain areas using tethered surgical instruments. Microrobots have the potential to greatly extend the accessibility to hard-to-reach locations within the human body to perform non-trivial tasks such as targeted therapy, removal of unwanted cells and drug deliverly to specific points inside the human body [1]. Soft microrobots have a lower density, are easy to fabricate and have a higher level of biocompatability compared to hard microrobots. Therefore, a soft microrobot (MagTwist) is modeled to determine its optimal geometry/frequency combination.

MagTwist consists of a flexible sheet with two permanent magnets at its edges. The permanent magnets are oriented perpendicular to the long axis of MagTwist and have opposite polarities, which can be seen in Figure 1. The deformation will be maximised under the influence of an external magnetic torque. By applying a magnetic field, the flexible sheet will twist. When the magnetic field rotates about the longitudinal axis of the sheet, it will swim by helical wave propagation. By using a rotating permanent magnet on the end of a robotic arm, these microrobots can be controlled inside the body [2]. Previous research focuses mainly on magnetic actuating of robots at microscale. So far, however, there has been little research on reconfigurable microrobots at mm-scale. The main research question of the paper is thereby: How to design a reconfigurable microrobot on mm-scale?

The main tasks are to optimise the MagTwist design and make the model based on the RST to calculate the velocity. Also, the results will be compared to the resistive-force theory (RFT). Furthermore, the MagTwist robot will be compared to already existing robots to discover if it is competitive. MagTwist could be made with only one side magnetic. It will be discussed how the MagTwist preforms with only one side made magnetic in comparison to two sides. This is necessary when MagTwist is scaled down to microscale, because of the likely inability to make both sides magnetic with two opposite polarities. At last the MagTwist should be produced and it will be investigated how the MagTwist can be produced on mm scale.

2 MODELING OF SOFT SHEET

The deformation of a soft sheet in low Reynolds numbers is governed by the balance between the drag, elastic, and magnetic moments. MagTwist is a soft

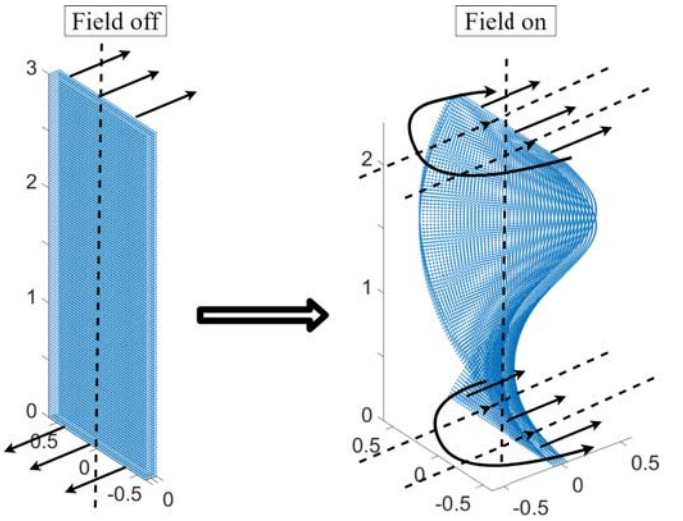

Figure 1: MagTwist, with the longitudal axis, magnetic field lines (dotted arrows) and polarity direction (solid line arrows)

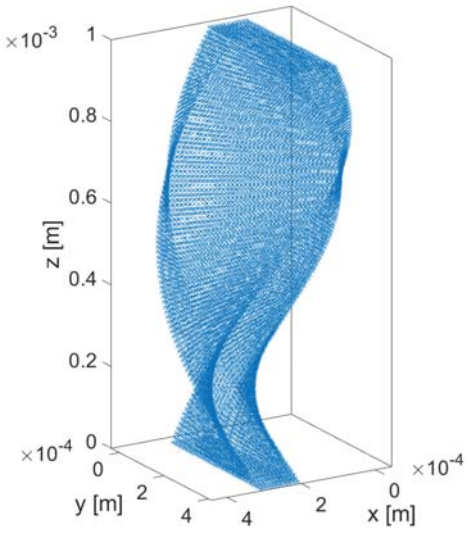

Figure 2: MagTwist is represented using a distribution of Stokeslets boundary points. The deformation of MagTwist about the z-axis is characterized by the angle of twist (π).

sheet and its time dependent deformation is modeled to analyze its ideal geometry. The other topics are answered by the use of literature.

2.1 Model definitions MagTwist

MagTwist has the following parameters which define its geometry: Length (L), width (W) and thickness (h). The ends are made magnetic. The length of this magnetic part is taken constant (0.2 mm) and has a magnetic saturation constant (M_s). Furthermore, the magnetic field strength (B) is varied form 0 to 20 mT. The magnetic field strength defines the maximum angular frequency of MagTwist. Thereby the actuation frequency is increased to the maximum frequency. The magnetic field also determines the angle of twist. The deformation of MagTwist is dictated by the balance between the elastic and drag moments under the influence of a fixed magnetic field. When the magnetic field is applied, MagTwist deforms and the balance between the drag and elastic moment governs the deformation. The magnetic field strength is constant during magnetic actuation. Therefore, MagTwist achieves rigid body rotation about its long axis and the geometry does not change when rotating. For calculating velocity, the RST equations are solved at low Reynolds numbers to ensure inertia terms can be neglected [3]. MagTwist is at mm-scale. To ensure low Reynolds numbers, silicon oil is taken as fluid because of its possible high viscosity (3.18 Pas) [3].

2.2 Rigid body Model

For calculating the RST equations , the geometry is needed. MagTwist is taken rigid. When rotating, it is assumed all points have the same position relative to each other. To realise the position vectors of points, equations (1) are used which describe two helices for the top half and bottom half of MagTwist.

$$\begin{aligned} x_{top} &= r sin(t) \\ y_{top} &= r cos(t) \\ x_{bottom} &= -r cos(t) \\ y_{bottom} &= -r sin(t) \\ z &= ct \end{aligned} \tag{1}$$

In equations (1), r is the radius of the helix, t is a vector between 0 and the angle of the deformation of MagTwist and c is a scalar which maps the helix onto the z-coordinate. By varying the width of the helix a grid can be created. Also, thickness is taken into consideration. Using a length of 1 mm, a width of 0.5 mm and a thickness of 0.1 mm, MagTwist is plotted in Figure 2. Because two sides are made magnetic, the max angle of twist is 180° [4].

Furthermore, for solving the RST equation, the velocity on each point is needed. To determine the velocity, MagTwist is rotated around the z-axis. The body is assumed rigid and thereby the velocity depending on the

center of rotation can be calculated using

$$\begin{aligned}\dot{\mathbf{r}}_\mathbf{n} &= \omega \times \mathbf{r}_\mathbf{n} \\ \omega &= [\omega_\mathbf{x}, \omega_\mathbf{y}, \omega_\mathbf{z}],\end{aligned} \tag{2}$$

where $\dot{\mathbf{r}}_\mathbf{n}$ is the velocity vector of n points, ω is the angular velocity and $\mathbf{r}_\mathbf{n}$ is the vector of the points mapped from the center of rotation.
Using the velocity vector, the traction forces on the surface can be calculated using

$$\mathbf{F_n} = \mathbf{G^{-1}}(\mathbf{r_n})(\dot{\mathbf{r}}_\mathbf{n} + \mathbf{v}) \tag{3}$$

The sum of F_n should be zero in the z-direction to ensure no acceleration. By an iterative process the velocity **v** is approximated. The regularised stokeslet **G**, is calculated using a specific cut-off equation. The **G** term in equation (4) is taken from [5]. It uses the einsteins summation convention

$$\begin{aligned}\mathbf{G}(\mathbf{r_n}) &= \frac{1}{8\pi\eta}\mathbf{G}^{\epsilon}_{\mathbf{ij}}(\mathbf{x}, \mathbf{x_0}) \\ =&\frac{1}{8\pi\eta}\left(\delta_{ij}\frac{\mathbf{r^2}+2\epsilon^2}{(\mathbf{r^2}+2\epsilon^2)^{3/2}} + \frac{(\mathbf{x_i}-\mathbf{x_{0,i}})(\mathbf{x_j}-\mathbf{x_{0,j}})}{(\mathbf{r^2}+2\epsilon^2)^{3/2}}\right),\end{aligned} \tag{4}$$

where **r** is $||\mathbf{x}-\mathbf{x}_0||$, η is viscosity and ϵ regulates the spread of the cut-off function. This term is depending on the distance between the boundary points (Δs) according to equation (5) as follows [6]:

$$\epsilon = 0.25\Delta s \tag{5}$$

This implies that when increasing the number of points, ϵ will decrease.

2.3 Second version of MagTwist for RST model

In the previous section, the model is dependent on the geometry of the boundary points given by equations (1). Another model was made. In this model, MagTwist shortens when twisted. The x and y coordinates are calculated using both a sine and cosine term to ensure an accurate circular twist. It is shown in Figure 1. Thereby this model is used in the continuation of the RST model.

2.4 Resistive-force theory

Another simple way to calculate the velocity of MagTwist is by the resistive-force theory (RFT) [4]. The x-component of total force which acts on the surface of MagTwist is

$$f = \int_0^L \int_{-W/2}^{W/2} \mathrm{d}F_x \mathrm{d}x\mathrm{d}y, \tag{6}$$

where *L* and *W* and the length and width of MagTwist. dF_x is the force acting on a small area and is

$$\begin{aligned}\mathrm{d}F_x = C_{dh}(Usin(\theta_y) + \omega ycos(\theta_y))sin(\theta_y) + \\ C_{dL}(Ucos(\theta_y) - \omega ysin(\theta_y))cos(\theta_y),\end{aligned} \tag{7}$$

where C_{dh} and C_{dL} are the local drag coefficients along the length and thickness direction, respectively. U is the velocity along the z-axis as shown in Figure 2. $\theta_y = y\frac{\mathrm{d}\theta}{\mathrm{d}x}$ and describes the angle of twist. It is determined numerically at each velocity, equation (6) is 0. The angle of MagTwist can be calculated using

$$\theta = \theta_{max}\frac{x}{L}, \tag{8}$$

where θ_{max} is the maximum angle of twist in radians.

2.5 Viscosity and magnetic field strength

To enhance the accuracy of the numerical model, the velocity of MagTwist should be dependant on the magnetic field strength and viscosity. The forces calculated in equation (4) scale with viscosity, but the forces cancel and the value of the force is thereby neglected. To calculated the maximum possible angular frequency of MagTwist (also called the cut-off frequency), the magnetic forces and drag torque should balance using

$$T_d + T_m = 0, \tag{9}$$

where T_d and T_m are the drag and magnetic torque, respectively. The angular velocity is calculated by extending equation (9) and rewriting for angular velocity which gives

$$\omega = \frac{|M||B|}{S\eta}, \tag{10}$$

where *M* and *B* are the magnetic moment and the magnetic field strength, respectively. By multiplying *M* with *B* as shown in equation (10), the magnetic torque

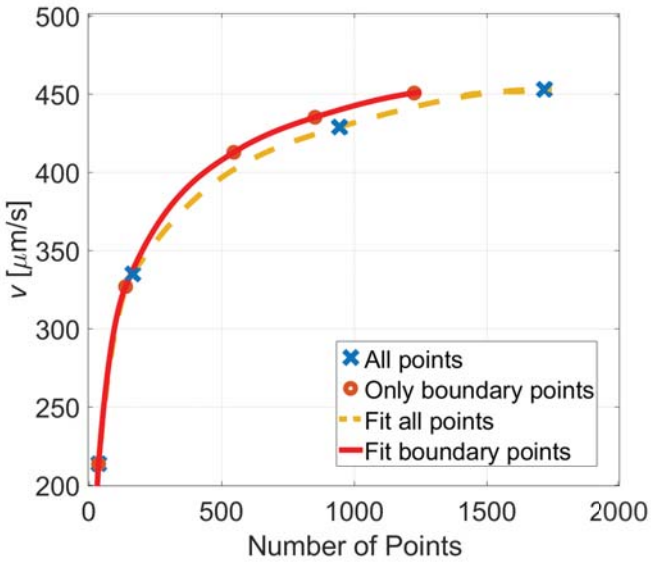

Figure 3: Accuracy of model for decreasing mesh density for only boundary points and all points

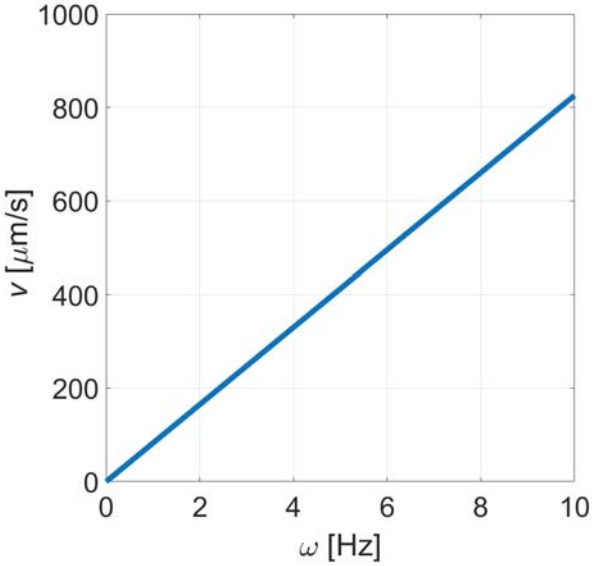

Figure 4: The linear velocity of MagTwist increases with the angular velocity linearly below the step-out frequency.

force is approximated. The magnetic saturation is calculated by multiplying the volume of the magnetic part with the magnetic saturation constant. S is the shape factor of the structure and is $12WL^2$ [4]. The angle of twist is calculated using [7]

$$\theta = \frac{|M||B|L}{JG}, \tag{11}$$

where L is the length of MagTwist, J is the torsion constant of a rectangular cross section [7] and G is the modulus of rigidity of the material. The magnetic field can be chosen freely but is limited to 20 mT. The shear modulus G is calculated for isotropic materials using [8]

$$G = \frac{E}{2(1+\nu)}, \tag{12}$$

where E is the Young's modules and ν is the Poisson ratio. The maximum frequency and angle of twist are used as input for the model.

2.6 Maximum stress

Under the influence of an external torque, the shear stress should not be larger than half of the yield strength for pure torsion [9]. The maximum shear stress is calculated using [7]

$$\tau_{max} = \frac{3T}{8ab^2}\left(1 + 0.6095\frac{b}{a} + 0.8865\left(\frac{b}{a}\right)^2 - 1.8023\left(\frac{b}{a}\right)^3 + 0.9100\left(\frac{b}{a}\right)^4\right), \tag{13}$$

where 2a is the width, 2b is the thickness and T is the torque force. Furthermore to verify the stress and angle calculations, an analysis in SolidWorks is done [10]. A model for MagTwist is made. Boundary conditions are needed for solving the FEM problem. At one side torque is applied on the magnetic part and on the other side the magnetic part is fixed.

3 NUMERICAL RESULTS

The rigid body model is evaluated. The robot has an angle of twist of 180°, a length of 1 mm, a width of 0.4 mm and a thickness of 0.2 mm. When increasing the number of points by decreasing Δs, the velocity of the model should convert to a finite value which can be seen in Figure 3. Furthermore, it can be seen that only taking the boundary points gives a more accurate value with less points. This is logical, because for solving the RST equations, only boundary points are needed. Thereby boundary points are used with $\Delta s = 0.0005$ (in Figure 3 at 546 points), to ensure

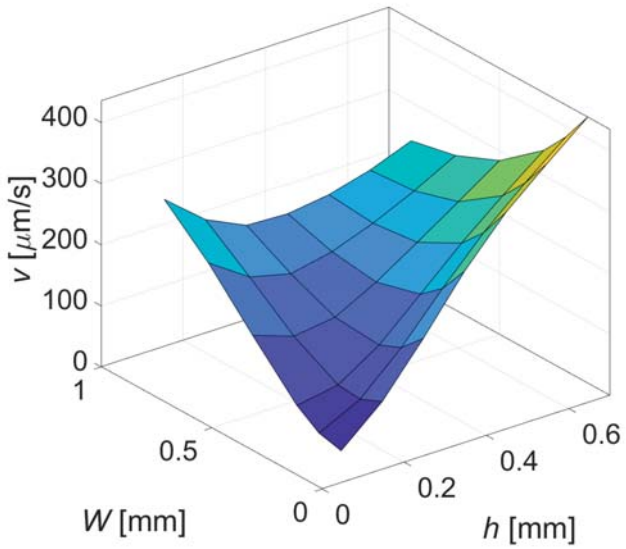

Figure 5: Varying width and thickness. The height/width ratio should be large to maximise velocity

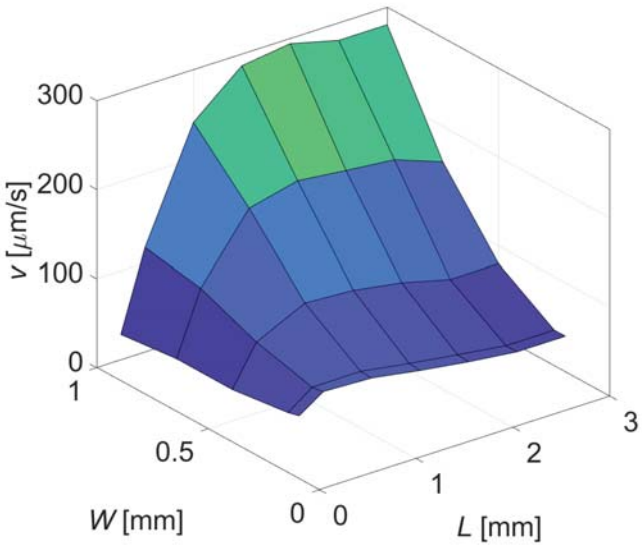

Figure 6: Varying width and length. The optimum lenght/width ratio is approximately 2

fast computation with an accuracy of approximately 90 % compared with the finest mesh.

3.1 Frequency response and angle variation

By increasing the rotation frequency, the velocity should increase. In Figure 7, it can be seen that the velocity increases linearly with the angular frequency. Furthermore, the angle of MagTwist is varied in Figure 7 with $\omega = 5$ Hz. For increasing the angle, the velocity of MagTwist increases. Two different MagTwist plots were tested. The first version uses equations (1) and the second version uses the second version of the model described in section 2.3. It can be seen in Figure 7, the second robot plot has a smaller velocity, but the shape of the line is similar. Version one is used till section 3.3. After section 3.3, version two is used.

3.2 Optimal Geometry of MagTwist

To find the optimal geometry to maximise the speed, various dimensions are tested and plotted in Figures 6 and 7. It can be seen in Figure 6 that the velocity increases with the length and then decreases. The velocity of MagTwist increases with the width and the thickness, as shown in Figure 5. It can be seen that the velocity increases with the width and decreases for the thickness, but when the thickness becomes large in comparison to the width, the velocity increases for thickness.

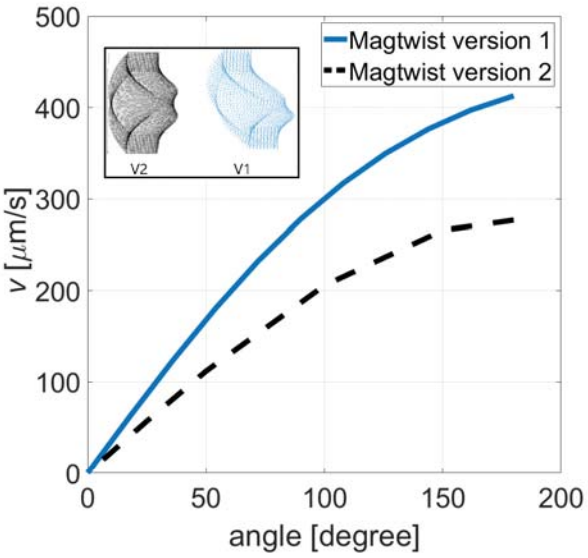

Figure 7: The swimming velocity for MagTwist version one and two at different angle of twists ($\omega = 5$ Hz)

3.3 Resistive-force theory

In equation (7), $C_{dh} = 2C_{dL}$ is initially used to calculate the velocity [4]. The drag coefficient is taken out of the integral and cannot be zero. Thereby for the sum of $\mathrm{d}F_x$ to be zero, the sum of the integral must be zero. When using an angle of twist of 180°, a length of 1 mm, a width of 0.4 mm and a angular frequency

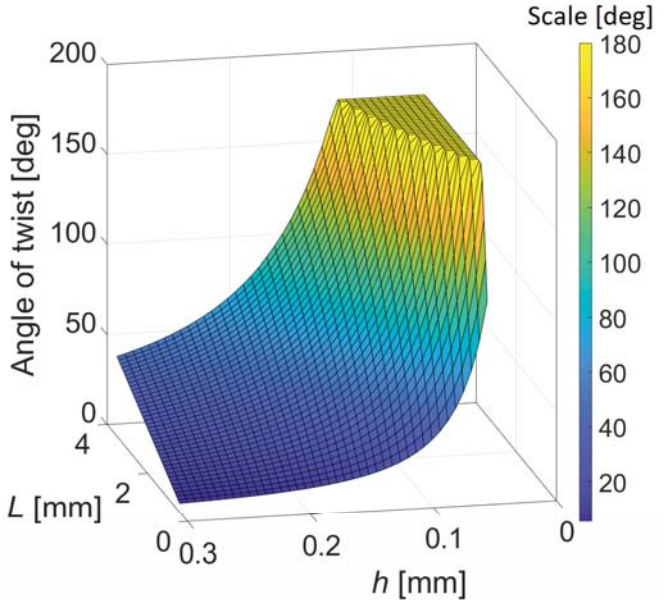

Figure 8: Angle of twist for varying length and thickness

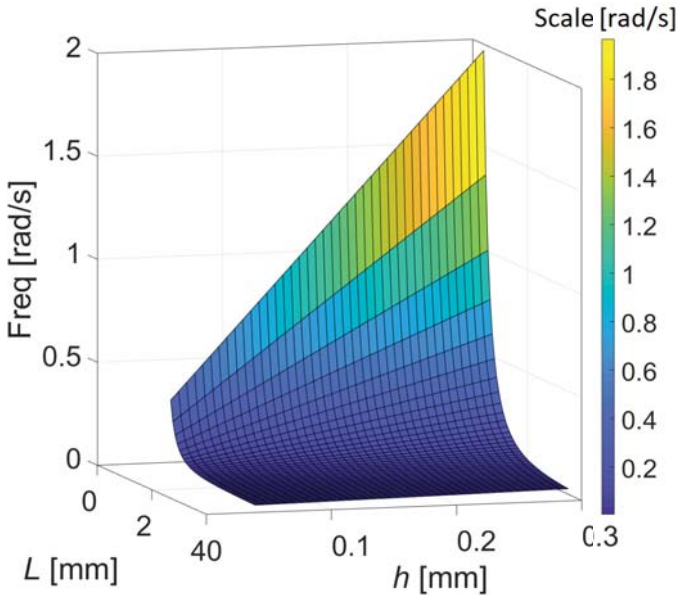

Figure 9: Cut-off frequency for varying length and thickness

of 5 Hz, the calculated velocity is 1.7 mm/s. When using $C_{dh} = 1.12C_{dL}$, the calculated velocity is 0.283 mm/s.

3.4 Influence of viscosity and magnetic field

In Figure 8 and Figure 9 the angle of twist and cut-off frequency are plotted for a magnetic field of 20 mT, a length of 0.2 mm for the magnetic part on both sides and a magnetic saturation constant of 62900 A/m [4]. The material chosen is silicone elastomer which has a Young's modulus of 0.205 MPa, a Poission ratio of 0.47 and a yield strength strength of 1.69 MPa [11]. The maximum allowable shear strength is approximately 1.69/2= 0.845 MPa. The length and thickness were varied with a width of 0.4 mm. The width was also investigated, but had limited impact and is thereby not shown. In Figure 8, the maximum alloable angle of twist is 180°.

3.5 Stress of MagTwist

The stress inside the material for a magnetic field of 20 mT and dimension: *L*=1 mm, *W*=0.4 mm and *H*=0.2 mm is 5.12 kPa when using equation (13). The resulted angle is 22.58° when using equation 11. When using Solidworks, the max stress is approximately 4.7 kPa and the angle is approximately 16° when looking at Figure 10.

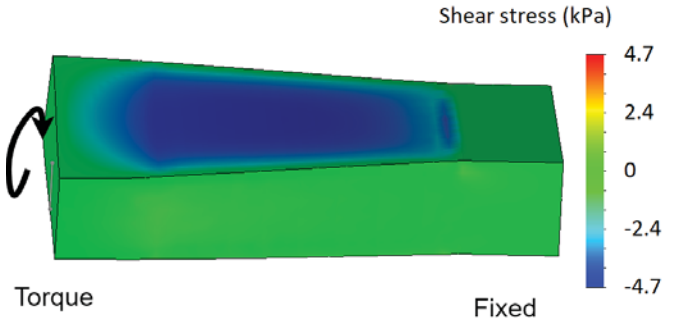

Figure 10: Stress analysis in Solidworks with torque boundary condition on left magnetic part and clamped boundary condition on the right magnetic part

3.6 Velocity for varying magnetic field

To realise an angle of twist of 180 °at 0.02 T, a length of 3 mm and a thickness of 0.1 mm is chosen (from Figure 11). To realise the highest velocity, the width must be larger than 1 mm based on the relation between the velocity and the width-length ration. By looking at Figure 6, the width is then taken 1.2 mm. The magnetic field is varied from 5 mT to 20 mT. The calculated velocity is shown in Figure 11. The maximum stress inside the material is 8.0×10^3 Pa for a magnetic field of 20 mT using equation (13).
Using the RFT described in Section 3.3 and $C_{dh} = 1.51C_{dL}$, the resulted velocity is 5.69×10^{-6} m/s at the cut-off frequency of 0.02 T (see Figure 11). The drag coefficient factor is determined by the RST. The factor is adapted till the RFT corresponds to the calculated

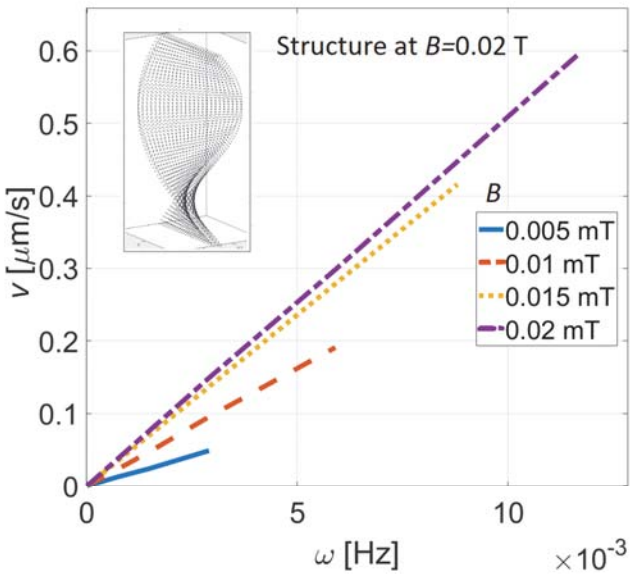

Figure 11: Velocity of MagTwist for varying magnetic field strength, plotted against the rotation frequency at viscosity =3.18 Pas

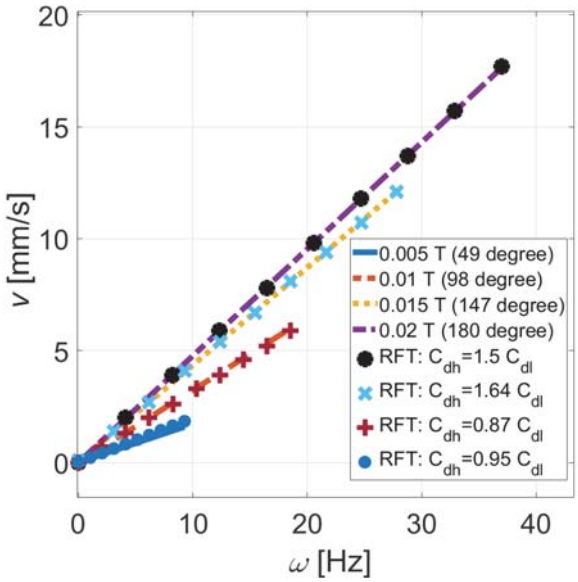

Figure 12: Velocity of MagTwist for varying magnetic field strength, plotted against the rotation frequency at viscosity =0.001 Pas, compared with RFT model

value in the RST. When using a viscosity of 0.001 Pas, the cut-off frequency increases as shown in Figure 12. In addition, the RST model and the RFT model are shown. At all magnetic field strengths, shortening of MagTwist is included in the RFT model by changing the length in equation (8). The length is taken from the RST model by looking at the plot of MagTwist at different magnetic field strengths.

4 DISCUSSION

The velocity of the calculations before section 3.3 are not accurate because of the first version MagTwist. Nevertheless, the shape of the equations and the conclusions drawn from then are still valid when looking at Figure 7.

4.1 Optimal Geometry of MagTwist

By varying the width and length, it can be seen in Figure 6, the length has an optimum value. The factor between these variables is approximately 2. When the width increases, also the optimum length becomes greater. This is due to the fact that increasing the length increases the drag force, but also the propulsion force. Furthermore, it can be seen when increasing the width in Figure 5, the velocity increases. This increase is expected because there is more surface area which generates a propulsive force. Further, when the width is low, the velocity becomes larger if the thickness increases. This is because the thickness becomes large in comparison to the width of MagTwist. This is most likely not possible. MagTwist can not have an angle of twist of 180° when the thickness is too high, because of high stresses. Thereby, to increase the velocity of MagTwist, the thickness must be taken small and width large.

4.2 Resistive-force theory

The velocity calculated by the RFT (0.0017 m/s) is relatively large in comparison with Figure 7. This is most likely due to the fact it is assumed $C_{dh} = 2C_{dL}$. When using $C_{dh} = 1.12C_{dL}$ the resulted velocity was more similar to Figure 7. For this specific geometry, the factor between the tangential drag coefficient and normal drag coefficient is thereby approximately 1.12.

4.3 Influence of magnetic field and viscosity

In Figure 11, it can be seen that the thickness should be minimised and the length be approximately 3 mm to ensure an angle of twist of 180°. Nevertheless the length of the magnetic part at the sides of MagTwist is taken constant and could be changed to optimise for the highest velocity. Furthermore, the shear modulus is calculated by equation (12) and is around 0.07 MPa for the silicone elastomer, but in the data sheet,

the shear modulus is 0.102 MPa [11]. This possible higher shear modulus has a negative effect on the angle of twist of MagTwist. When using this higher shear modulus, a thickness of 0.08 mm is necessary to archive an angle of twist of 180°. Still, a thickness of 0.1 mm is used in the remaining of the thesis. When looking at Figure 9, it can be seen the cut-off frequency is low at large lengths. This is the result of the high viscosity, which is present in equation (10). The cut-off frequency also decreases when the thickness decreases. This is due to the fact that the magnetic volume decreases and thereby lowering the torque force. To ensure a higher frequency, a larger magnetic field should be used or a fluid which has a lower viscosity.

4.4 Stress and angle of twist

The stress is calculated in two different ways. The resulting shear stress is similar. Thereby it is concluded equation (13) can calculate the shear stress inside MagTwist accurately. For the specific geometry and magnetic field, the stresses inside the material are small and MagTwist will not fail. The angle of twist differs, but this is most likely the result of the modeling of MagTwist. In the solidworks model, the torsion force is applied on the whole magnetic part and not at the ends of the robot. Thereby the length of the robot decreases and the angle of twist also decreases. When taking a larger length, this difference in angle will decrease.

4.5 Velocity for varying magnetic field

The optimisation of MagTwist is not ideal. The value used for the optimal width for a length of 3 mm is 1.2 mm, which gives a ratio of 2.5. The optimum ratio between the length and width is around 2 when looking at Figure 6 more extensively. Nevertheless, it has limited impact on the optimisation because MagTwist shortens. When taking into account the shortening of MagTwist, the ratio becomes 1.94 at 0.02 T, which is close to 2. Therefore, it is assumed this width of MagTwist is optimised enough. It should be noted that the shortening of MagTwist is different for each magnetic field strength. This means there is not an ideal length for all magnetic field strengths. When looking at Figure 11, it can be seen that the velocity increases for increasing magnetic field strengths. This is the result of a higher cut-off frequency and greater angle of twist of MagTwist. Nevertheless the cut-off frequency is low, because of the large viscosity of silicon oil. When using the RFT method described in Section 3.3, the velocity corresponds when using a factor of 1.5 between the drag coefficient in the length and longitudinal direction. When using a viscosity of 0.001 Pas, the velocity between the RFT and regularized stokes solutions correspond when using a factor of 1.51 at a magnetic field of 0.02 T. Looking at Figure 12, it can be seen that for specific drag coefficients, the RFT and RST models correspond. Nevertheless, these values are only valid for the specific geometry of the structure. Also, the RFT model does not consider the cut-off frequency. This is the result of the RST model. Nevertheless it is interesting to see the two models are given similar answers for the velocity.

4.6 Rigid model

It is assumed the MagTwist is rigid, but when turning in a fluid the drag forces have influence on the shape and thereby the velocity of the robot. To increase the accuracy of the model, a flexible MagTwist can be investigated in further research.

4.7 Comparison with other microrobots

When comparing the MagTwist to other microrobots, a few thing stand out. MagTwist can propel itself in two directions. Some of already existing microrobots, do not have this ability, but there is for instance a sperm like robot with two flagella which can also achieve bidirectional motion [12]. Furthermore, the speeds of MagTwist is relatively high. Another microrobot which uses jelly fish like propulsion [13], has similar dimensions and can achieve a velocity of 4 mm/s at a viscosity of 0.005 Pas. The velocity of MagTwist is higher, but not tested at a viscosity of 0.005 Pas. Also, a microrobot which uses acoustical propulsion can archive a velocity of 90 body lengths per second at low viscosity [14]. This is higher than MagTwist (approximately 5-6 body lengths per second), but the absolute velocity of MagTwist is higher, due to the larger scale of the robot. Furthermore, a one-tailed sperm like microrobot could archive a speed of 0.06 body length per seconds at a viscosity of 0.95 Pas [12]. This viscosity is high and thereby the velocity cannot be compared directly. Concluding, it seems the MagTwist Robot has reasonable performance when looking at propulsion speed.

4.8 *Comparing with only one side made magnetic*

Although only the two sides of the magnetic field are modeled, MagTwist could also be made with only one side made magnetic. By turning the magnetic field, the structure will form a helix because of the drag forces. The structure is thereby not limited to the maximum angle of 180°. Nevertheless, two sides made magnetic, makes it possible to move backwards. Also, it is possible to grab for instance medicine or tissue. Furthermore, it is not possible to adapt the angle of twist for different fluids, while changing the angular frequency of MagTwist when only one side is magnetic [4]. Thereby, making MagTwist with both sides magnetic is the best option.

4.9 *Fabrication of MagTwist*

Various microrobots are produced by 3D printing[15]. Possible 3D production teqniques are inkt-jet printing or photolithography [4]. Thereby it is expected, MagTwist could also be 3D printed. Other means of production could also be feasible. Extrusion looks like a promising option. It could continuously produce small robots at high speed. For magnetisation of the sides, small magnets could be used or the sides could be made magnetic by an external magnetic field. To achieve opposing polarities, one side must be shielded from the magnetic field during magnetisation and this step is repeated for the other side [4].

5 CONCLUSIONS

The swimming velocity of MagTwist is dependent on various parameters such as the width-length ratio, thickness, magnetic moment and magnetic field strength. There exist an optimal ratio of approximately 2 between the length and width of MagTwist. The optimal angle of twist is 180° and results in a swimming speed of 5-6 body length per second for the optimised geometry. A relatively high magnetic field is desirable to enhance the propulsion, but is limited to 20 mT. To ensure a twist of 180° at 20 mT, the thickness should be 0.1 mm and the length 3 mm. A optimal width of 1.2 mm is chosen. The magnetic field is rotated and MagTwist rotates in sync with the magnetic field below the cut-off frequency. To approximate the velocity of the MagTwist using the RFT, the factor between the longitudinal and tangential drag coefficient for the specific geometry is approximately 1.5 for angle of twist of 180°. To achieve a high cut-off-frequency, the magnetic field should be higher than 20 mT or the viscosity must be low. The stresses in the material are approximated and based on these calculations, MagTwist will not exceed the stress limit. The highest velocity of 17.7 mm/s is achieved at a viscosity of 0.001 Pas and a magnetic field of 20 mT which makes MagTwist an efficient soft swimmer compared to other magnetically driven helical microrobots.

5.1 *Future work*

Higher magnetic field strength could be investigated in further research to archieve a higher cut-off frequency at a higher viscosity. A possible approach for achieving a higher magnetic field is by using a robotic arms with magnets on the end. Further research could also focus on making the MagTwist non-rigid and thereby depending on the forces of the fluid. Also, the optimisation is rough. The ideal width, thickness and magnetic part of MagTwist could be further investigated and could be further optimised for specific applications. At last, MagTwist can be produced and tested in the laboratory with an appropriate material.

REFERENCES

1. B. J. Nelson, I. K. Kaliakatsos, and J. J. Abbott. Microrobots for minimally invasive medicine. *Annual Review of Biomedical Engineering*, 12:55–85, 2010.
2. T. W. R. Fountain, P. V. Kailat, and J. J. Abbott. Wireless control of magnetic helical microrobots using a rotating-permanent-magnet manipulator. In *Proceedings - IEEE International Conference on Robotics and Automation*, pages 576–581, 2010.
3. T. S. Yu, E. Lauga, and A. E. Hosoi. Experimental investigations of elastic tail propulsion at low reynolds number. *Physics of Fluids*, 18(9), 2006.
4. S. Namdeo, S. N. Khaderi, and P. R. Onck. Numerical modelling of chirality-induced bidirectional swimming of artificial flagella. *Proceedings of the Royal Society A: Mathematical, Physical and Engineering Sciences*, 470(2162), 2014.
5. R. Cortez, L. Fauci, and A. Medovikov. The method of regularized stokeslets in three dimen-

sions: Analysis, validation, and application to helical swimming. *Physics of Fluids*, 17(3), 2005.
6. I. S. M. Khalil, A. Klingner, V. Magdanz, F. Striggow, M. Medina-Sánchez, O. G. Schmidt, and S.k Misra. Modeling of spermbots in a viscous colloidal suspension. *Advanced Theory and Simulations*, 2(8), 2019.
7. W. C. Young and R.G. Budynas. *Roark's Formulas for Stress and Strain*. McGraw-Hill, 2002.
8. F. P. Beer and E. R. Johnston. *Mechanics of Materials*. McGraw-hill, 1992.
9. J. Kerns. What's the difference between failure theories? `https://www.machinedesign.com/learning-resources/whats-the-difference-between/article/21834909/whats-the-\difference-between-failure-theories`, 11-10-2016. Accessed on: 2-6-2020.
10. Dassault Systèmes SolidWorks Corporation. Solidworks 2019. 2019.
11. Granta Design Limited. CES 2019 education edition. 2019.
12. I. S. M. Khalil, A. F. Tabak, Y. Hamed, M. E. Mitwally, M. Tawakol, A. Klingner, and M. Sitti. Swimming back and forth using planar flagellar propulsion at low reynolds numbers. *Advanced Science*, 5(2), 2018.
13. M. Su, T. Xu, Z. Lai, C. Huang, J. Liu, and X. Wu. Double-modal locomotion and application of soft cruciform thin-film microrobot. *IEEE Robotics and Automation Letters*, 5(2):806–812, 2020.
14. A. Aghakhani, O. Yasa, P. Wrede, and M. Sitti. Acoustically powered surface-slipping mobile microrobots. *Proceedings of the National Academy of Sciences of the United States of America*, 117(7):3469–3477, 2020.
15. R. Bernasconi, E. Carrara, M. Hoop, F. Mushtaq, X. Chen, B. J. Nelson, S. Pané, C. Credi, M Levi, and L. Magagnin. Magnetically navigable 3d printed multifunctional microdevices for environmental applications. *Additive Manufacturing*, 28:127–135, 2019.